INTERNATIONAL JOURNAL FOR NUMERICAL METHODS IN FLUIDS
Int. J. Numer. Meth. Fluids 2008; **57**:1545–1568
Published online 16 January 2008 in Wiley InterScience (www.interscience.wiley.com). DOI: 10.1002/fld.1695

Least-squares finite element processes in h, p, k mathematical and computational framework for a non-linear conservation law

K. S. Surana[1,*,†], S. Allu[1], J. N. Reddy[2] and P. W. Tenpas[1]

[1]*Department of Mechanical Engineering, The University of Kansas, 3013 Learned Hall, Lawrence, KS 66045-2234, U.S.A.*
[2]*Department of Mechanical Engineering, Texas A&M University, College Station, TX 77843-3123, U.S.A.*

SUMMARY

This paper considers numerical simulation of time-dependent non-linear partial differential equation resulting from a single non-linear conservation law in h, p, k mathematical and computational framework in which $k=(k_1, k_2)$ are the orders of the approximation spaces in space and time yielding global differentiability of orders (k_1-1) and (k_2-1) in space and time (hence k-version of finite element method) using space–time marching process. Time-dependent viscous Burgers equation is used as a specific model problem that has physical mechanism for viscous dissipation and its theoretical solutions are analytic. The inviscid form, on the other hand, assumes zero viscosity and as a consequence its solutions are non-analytic as well as non-unique (*Russ. Math. Surv.* 1962; **17**(3):145–146; *Russ. Math. Surv.* 1960; **15**(6):53–111). In references (*Russ. Math. Surv.* 1962; **17**(3):145–146; *Russ. Math. Surv.* 1960; **15**(6):53–111) authors demonstrated that the solutions of inviscid Burgers equations can only be approached within a limiting process in which viscosity approaches zero. Many approaches based on artificial viscosity have been published to accomplish this including more recent work on $H(\mathrm{Div})$ least-squares approach (*Commun. Pure Appl. Math.* 1965; **18**:697–715) in which artificial viscosity is a function of spatial discretization, which diminishes with progressively refined discretizations. The thrust of the present work is to point out that: (1) viscous form of the Burgers equation already has the essential mechanism of viscosity (which is physical), (2) with progressively increasing Reynolds (*Re*) number (thereby progressively reduced viscosity) the solutions approach that of the inviscid form, (3) it is possible to compute numerical solutions for any *Re* number (finite) within *hpk* framework and space–time least-squares processes, (4) the space–time residual functional converges monotonically and that it is possible to achieve the desired accuracy, (5) space–time, time marching processes utilizing a single space–time strip are computationally efficient. It is shown that viscous form of the Burgers equation without linearizing provides a physical and viable

*Correspondence to: K. S. Surana, Department of Mechanical Engineering, The University of Kansas, 3013 Learned Hall, Lawrence, KS 66045-2234, U.S.A.
†E-mail: kssurana@ku.edu

Contract/grant sponsor: DEPSCoR, AFOSR and WPAFB; contract/grant numbers: F49620-03-1-0298, F49620-03-1-0201

mechanism for approaching the solutions of inviscid form with progressively increasing *Re*. Numerical studies are presented and the computed solutions are compared with published work. Copyright © 2008 John Wiley & Sons, Ltd.

Received 31 July 2006; Accepted 23 October 2007

KEY WORDS: least squares; finite element; variational consistency; time-dependent Burgers equation

1. INTRODUCTION

1.1. Literature review

In this section we present a review of published work on the numerical computations of the solutions of linear and non-linear hyperbolic and parabolic differential and partial differential equations. The idea of generalized solutions of the differential and partial differential equations was first proposed by S. L. Sobolev and constitutes the mathematics and thus the backbone of the finite element method in conjunction with variational methods. In an important paper Godunov [1] discussed the problem of generalized solutions of quasi-linear equations in gas dynamics. The author illustrated that for $\partial\varphi/\partial t+\varphi\partial\varphi/\partial x=0$ (inviscid Burgers equation), the theory of generalized solutions leads to non-uniqueness. This situation can be corrected by imposing additional restriction on the weak form. For the Burgers equation (and its generalization to quasi-linear systems), this restriction leads to the law of conservation of entropy. Thus, in gas dynamics equations describing reversible processes, the law of conservation of entropy must hold in the theory of generalized solutions, whereas in irreversible processes there must be entropy production which in physical systems under adiabatic conditions is only possible through dissipative mechanisms. In other words, in the theory of generalized solutions of gas dynamics equations, the law of increase in entropy must be replaced by the law of dissipation of energy to ensure the uniqueness of generalized solutions. A rigorous mathematical exposition of the solutions of quasi-linear hyperbolic equations is presented by Rozhdestvenskii [2]. The findings are similar to those reported by Godunov and are summarized in Reference [3]. The author shows that systems of linear equations are always conservative, while the systems of non-linear equations, generally speaking, are conservative only for $n\leqslant 2$ (two conservation laws).

Solution of non-linear hyperbolic systems has also been reported by Grimm [4] and Smoller [5, 6]. Grimm proposed an existence theorem and provided its proof. Smoller reported general characteristics of these solutions with specific details and discussion of the Riemann problem and contact discontinuities. Hopf [7] presented a mathematical proof of the convergence of weak solutions of quasi-linear equations of first order with artificial viscosity to strong solutions as viscosity approaches zero. Friedrichs and Lax [8] discussed first-order conservative systems of non-linear conservation laws which have as a consequence an additional conservation law. They show that if the additional conserved quantity is a convex function of the original ones, the original system can be put into symmetric hyperbolic form. They also derive an entropy inequality, which has also been suggested by Kruzhkov [9] for discontinuous solutions of the given system of conservation laws. Existence of discrete shocks, genuine non-linearity and the use of fourth-order dissipation in a single conservation law have been reported by Mock [10, 11]. A thorough mathematical exposition with theorems and proofs for uniqueness of the solutions of hyperbolic conservation laws has been

DOI: 10.1002/fld

reported by Diperna [12]. Existence and uniqueness of entropy solutions to the Riemann problem for hyperbolic systems of two conservation laws has been reported by Keyfitz and Kranzer [13]. The paper presents proofs of existence and uniqueness of the solutions in one space variable. Only strictly hyperbolic and genuinely non-linear systems are investigated. Noh [14] reported an investigation of the errors introduced in the calculation of strong shocks using artificial viscosity of the type in Reference [15] and artificial heat flux. An investigation of the errors introduced in the interaction of strong shocks due to the assumption of finite shock width has been reported by Menikoff [16].

There are many published works addressing numerical simulation of partial differential equations resulting from non-linear hyperbolic conservation laws. Here, we primarily consider finite element approaches. Comprehensive literature review of published finite element approaches for convection–diffusion and Burgers equation can be found in References [17, 18]. As pointed out in Reference [2], for linear and non-linear hyperbolic systems based on one or two conservation laws it is possible to show the convergence of generalized solutions to strong solutions.

The 1-D form of the time-dependent momentum equation yields 1-D time-dependent viscous form of the Burgers equation, which when non-dimensionalized contains the dimensionless parameter, Reynolds (Re) number. The viscosity of the medium is reflected in Re. For the viscous form of the Burgers equation, the solutions are analytic with finite shock width dependent on the Re number. For higher Re, the shock width is approximately $O(1/Re)$ and hence remains finite for a finite value of Re. The shock structure resolution in this case requires prudent mesh refinements in the shock zone to accommodate the localized high gradients of the solution for high Re. The analytic solutions of the viscous form of the Burgers equation can be expressed in terms of infinite series expansion in space and time. Obviously, the best way to simulate such a solution is to use a single space–time element with p-levels in space and time approaching infinity, which of course is not possible. Thus, if we limit p-levels in space and time, then obviously discretization of the domain in space and time is necessary. For the converged numerical solutions to approach theoretical solutions (up to certain order derivatives), higher-order global differentiability (smoothness) of local approximation in space and time is desirable. Hence, h, p, k mathematical framework may be beneficial for numerical simulation of such processes.

Inviscid form of the Burgers equation is a special case of the viscous form in which $Re=\infty$ (zero viscosity). In this case, shock width $O(1/Re)$ becomes zero and we have a prefect shock, i.e. jump with non-unique values of the solution at the shock. Such solutions are non-analytic and singular at the shock and therefore the solution derivatives are not defined at the shock. These solutions cannot be simulated in this precise form using finite element processes employing local approximations of class C^0. As pointed out in Reference [1] an attempt to compute solutions of inviscid Burgers equation would lead to non-uniqueness of the solution and hence obviously the lack of convergence of the associated functionals (for example, residual functional in least-squares processes). The solutions of the inviscid Burgers equations can only be approached as a limiting case. For example:

(i) Artificial viscosity approach [1] in which case one shows that as the artificial viscosity approaches zero the solutions of the inviscid form can be visualized (but not possible to compute).
(ii) More recently, $H(\mathrm{Div})$ least-squares processes have been used in which the inviscid Burgers equation is recast as a first-order system of coupled partial differential equations using auxiliary variables [3, 19, 20]. The authors recognize the non-uniqueness of the solution and

DOI: 10.1002/fld

lack of existence of unique first derivative at the shock and introduce the Frêchet derivative to restore analyticity of the solution. Many theorems related to the convergence of the least-squares functional, uniqueness of the solution of the reconstructed initial value problem (IVP) and convergence of its weak solutions are presented. Some significant points are worth noting: (a) As pointed out by Godunov [1], the solutions of inviscid Burgers equations are non-unique and the uniqueness can only be restored by introducing some mechanism of viscosity (artificial or physical). (b) In the $H(\mathrm{Div})$ approach, mesh-dependent artificial viscosity is introduced in the inviscid form of the Burgers equation such that progressively refined meshes in the spatial direction yield progressively decreasing viscous dissipation mechanism and hence it is possible to argue that in the limit the discretization length in space approaches zero, the solutions of the inviscid Burgers equations are possible to approach (but never possible to compute directly). (c) From (b) it is clear that in References [3, 19, 20] the authors only solve the viscous form of the Burgers equation in which the mechanism of viscous dissipation is artificial (non-physical) and not the inviscid form. (d) The viscous form of the Burgers equation resulting form the non-linear conservation law already has a physical mechanism of viscous dissipation which in the dimensionless form of the GDE is intrinsic in the *Re* number. (e) In view of (a)–(d) it is quite clear that here we have two possible propositions. Should the solutions of the inviscid Burgers equation be approached using the artificial viscosity approach (let it be $H(\mathrm{Div})$ or any other) or should these be approached using viscous form of the GDE with progressively increasing *Re* thereby progressively diminishing viscosity. First, we argue that the viscous form of the Burgers equation has a physical mechanism of viscosity and its solutions are always unique and that the computations using this form require no other artificial means. Secondly, we must show that the computations for the viscous form are possible with monotonic convergence of the least-squares functional, accurate resolutions of the shock structure (depending upon *Re*) for discretizations that are no more refined than those employed in the artificial viscosity approaches (hence computationally competitive). For a given *Re*, the computed evolution is always time accurate and as *Re* is increased progressively the computed solutions indeed approach those of the inviscid form. (f) In Reference [3] the solutions reported using $H(\mathrm{Div})$ approach for $16\times16, 32\times32, 64\times64$ and 256×256 space–time meshes show that these solutions correspond to progressively increasing *Re*; however, from this approach *Re* corresponding to these solutions cannot be quantified.

We remark that if we are to diffuse the solutions in some form or the other, then, we may as well use the viscous form of the Burgers equation in which the diffusion is physical due to viscosity of the medium and is reflected in the *Re* number. In this approach if one could show that:

(a) The solutions remain unique and convergent for any finite *Re* number.
(b) The associated least-squares functional shows monotonic convergence and indeed approaches zero.
(c) For progressively increasing *Re* the progressively reduced shock width ($O(1/Re)$) for high *Re* is achieved and that the computations are always time accurate then, we indeed have a computational strategy in which the solutions of the inviscid Burgers equation can be visualized as a limiting case when *Re* approaches infinity. This approach is much more appealing because of the fact that viscous form of the Burgers equation is in agreement with the physics, and, that it requires no other treatments to regularize singular solutions as

DOI: 10.1002/fld

in case of the inviscid Burgers equation, as they are naturally analytic due to the physics of the viscous medium. We address these issues in the paper.

1.2. Global smoothness or differentiability of approximations

Just like in boundary value problem (BVP), in IVPs also, continuity, differentiability and order of global differentiability of the dependent variables in space and time are dependent on physics. When the theoretical solutions of the IVP are analytic, the derivatives of the dependent variables of up to orders 'j' $=(j_1, j_2)$ in space and time are continuous, differentiable and bounded, where j_1, j_2 approaching infinity are admissible. When one approximates numerical solutions of the IVP, the global smoothness of the approximations up to any desired order in space and time in the point-wise sense is necessary if the approximations are to approach theoretical solutions in terms of continuity and global differentiability up to a desired order.

The issue and importance of global smoothness of computed solutions in finite element processes is not new. In the classical paper, Strang [21] points out the intrinsic weakness of C^0 basis functions (non-conforming elements) for BVP where they produce jump in the first derivative normal to the inter-element boundaries, and hence, provide a measure of deviation of the computed solution from C^1 behavior. In another classic paper [22], Irons suggested that if such elements pass the 'patch test', then the weak convergence of the class C^0 to C^1 is assured. Subsequently, Strang [21] showed mathematically that this indeed is the case. Strang [21] points out that in the numerical approximations for BVP with inter-element discontinuity of the first derivative, the strain energy becomes unbounded and thus such basis functions are not admissible in the true mathematical sense. However, based on the theory of distribution and the concept of generalized derivative, the strain energy remains finite when the integrals are in Lebesgue sense. It is clear that, even though C^0 basis functions may yield weak convergence to class C^1 using h, p, hp adaptive processes, this issue of weak convergence or lack of it can be completely avoided by employing the basis functions of class C^1 or higher (if needed) in the integral forms to begin with.

Discussions of global smoothness for BVP can also be found in References [23, 24] among many others. To some extent, global smoothness has been recognized as an important aspect in all numerical computations; however, very little has been done to design computational processes in which higher order of global smoothness is intrinsically incorporated in the computational processes. The majority of published work, using Galerkin, mixed Galerkin, least squares, space–time least-squares processes (STLSP) among many other computational techniques, is strictly based on C^0 local approximations in space as well as time with perhaps only a few exceptions. Hermit basis functions and Hermite finite elements based on these functions have been used in solid mechanics and other areas. A comprehensive literature review of these can be found in [25]. Katz and Wang [26], Wang *et al*. [27] and Wang [28] have presented p-version of finite element method with C^1 basis functions for a triangular element to solve a bi-harmonic equation. Other references to C^1 continuity across inter-sub domain boundaries may be found in References [29–33].

More recently, while solving gas dynamics equations numerically using space–time least-squares finite element method with p-version C^{00} basis functions in space and time, Surana and Van Dyne [34–36] and Nayak [37] noted the presence of discontinuities in the first normal derivatives of dependent variables at the inter-element boundaries, which are always present in the weakly converged solutions. These discontinuities generate solution perturbations that amplify as one marches in time (time evolution) and eventually leads to the failure of the computational processes. This problem was eliminated by using C^{11} basis functions in space and time, thereby enforcing

DOI: 10.1002/fld

continuity of the first normal derivatives of dependent variables at the inter-sub domain boundaries in the strong sense. The necessity and merits of using C^{11} basis functions in 2-D incompressible flows of Newtonian and polymer flows have been reported by Nayak [37]. Surana and Bona reported solutions of class C^1 and C^{11} [38] for stationary and transient 1-D convection–diffusion and Burgers equations. Tremendous success of C^1 and C^{11} basis functions in BVP and IVP provided the motivation for generalization of these concepts, which eventually led to the research work presented by Surana *et al*. [39–42] in which the authors have presented development of a new mathematical and computational framework for BVP based on h, p, k as parameters influencing all finite element computations and variational consistency of the integral forms. In a more recent paper Surana *et al.* [42] have presented k-version of finite element method for IVP based on h, p, k mathematical framework and space–time variational consistency (STVC) of the space–time integral forms. The space–time decoupled methods were not considered for obvious reasons and space–time coupled processes are advocated to be the preferred approach. The authors show space–time, time marching process to be meritorious and superior to space–time meshes in all aspects. The authors classify all space–time differential operators over a space–time strip into two categories: non-self adjoint and non-linear, and show space–time Galerkin method and Galerkin method weak form to be space–time variationally inconsistent whereas STLSP are space–time variationally consistent and hence meritorious in all aspects.The importance of variational consistency for BVP and STVC for IVP stems from the fact that such integral forms yield computational processes that are unconditionally non-degenerate and for IVP the issues related to Courant–Friedrichs–Lewy (CFL) number and stability are completely eliminated.

1.3. Scope of the present work

The theoretical solutions of the viscous form of the time-dependent Burgers equation are of higher-order global differentiability in space and time. It is shown that in h, p, k mathematical framework, the solutions of the inviscid Burgers equation are approached with progressively increasing *Re* number and order $k = (k1, k2)$; $k1$ and $k2$ being the orders of the approximation space in space and time. Minimally conforming spaces in space and time are established and the need for spaces of orders higher than minimally conforming is clearly demonstrated. Details are presented to establish uniqueness of the numerical solutions from the STLSP in h, p, k framework when using second-order GDEs (as opposed to a system of two first-order GDEs) and Newton's linear method with line search for solving the resulting system of non-linear algebraic equations. In the STLSP non-linear GDEs are utilized without linearization or any other assumptions that the least-squares functional and its first variation correspond to the actual non-linear GDEs. Numerical studies are presented to demonstrate all mathematical and computational features of the proposed framework and the numerical results are compared with the published work.

2. TRANSIENT 1-D BURGERS EQUATION

2.1. Mathematical and computational framework

The details of h, p, k mathematical and computational framework for IVP and the importance of space–time variationally consistent integral forms have been presented by Surana *et al*. [42]. The concepts pertinent in context with the present work are described briefly in the following.

DOI: 10.1002/fld

Let $A\varphi - f = 0$ in $\Omega_{xt} = \Omega_x \times \Omega_t = \Omega_x \times (0, \tau)$ be an abstract IVP in which A is a space–time differential operator. Then, all space–time differential operators A can be classified mathematically over $\bar{\Omega}_{xt}$ or ${}^n\bar{\Omega}_{xt}$ ($\bar{\Omega}_{xt} = \bigcup_n {}^n\bar{\Omega}_{xt}$), an nth space–time strip into two categories: non-self adjoint or non-linear. Using this classification STVC and space–time variational inconsistency (STVIC) of the space–time methods of approximation such as space–time Galerkin method, Galerkin method/weak form, Petrov–Galerkin method, weighted residual method and least-squares processes can be established (see Reference [42] for the definition of STVC, STVIC and other details) over a space–time strip or the entire space–time domain. STVC space–time integral form yields an unconditionally stable and non-degenerate computational process regardless of the choices of h, p and k and the dimensionless parameters in the description of the IVP during the entire evolution. On the other hand, STVIC space–time integral forms do not ensure unconditionally stable and non-degenerate computational processes for all choices of h, p, k. Authors in Reference [42] have shown that all other space–time methods of approximation except space–time least-squares processes (STLSP) are STVIC for both classes of space–time differential operators. STLSP yield STVC space–time integral forms for both classes of differential operators and hence are worthy of consideration as a general computational methodology for all IVP, and hence will be considered in the present work.

Space–time integral forms for a space–time strip with time marching are meritorious in terms of computational efficiency and error control due to the fact that evolution is time marched only when converged solution is achieved for the existing space–time strip or slab and hence, will be considered in this work.

The concept of global differentiability of approximation φ_h, k-version of finite element method and k, hk, pk, hpk processes were introduced by Surana *et al.* [39–41] for self-adjoint, non-self-adjoint and non-linear differential operators in BVP. These concepts were further extended for IVP in Reference [42].

Let the space–time differential operator A in $A\varphi - f = 0$ in Ω_{xt} contain derivatives of up to orders $2m_1$ in space and up to orders $2m_2$ in time. Let $\bar{\Omega}_{xt}^{\mathrm{T}} = \bigcup_{n=1}^{n^*} (\bigcup_{e=1}^{M} {}^n\bar{\Omega}_{xt}^e)$ be a discretization of space–time domain $\bar{\Omega}_{xt}$ in which n^* is the number of space–time strips, M is the number of space–time elements in a space–time strip and ${}^n\bar{\Omega}_{xt}^e$ is the space–time element 'e' for the nth space–time strip. Let $\varphi_h(x,t)$ be an approximation of φ in $\bar{\Omega}_{xt}^{\mathrm{T}}$ and let ${}^n\varphi_h^e$ be an approximation of $\varphi(x,t)$ in ${}^n\bar{\Omega}_{xt}^e$; then, we have,

$$\varphi_h(x,t) = \bigcup_{n=1}^{n^*} \left(\bigcup_{e=1}^{M} {}^n\varphi_h^e(x,t) \right) \tag{1}$$

and the following holds:

(a) If $A\varphi_h(x,t) - f = E \ \forall x, t \in \bar{\Omega}_{xt}^{\mathrm{T}}$, then $\varphi_h \in H^k(\bar{\Omega}_{xt}^{\mathrm{T}})$, $k = (k_1, k_2)$, $k_1 \geqslant 2m_1 + 1$, $k_2 \geqslant 2m_2 + 1$ in which k_1 and k_2 are orders of the scalar product space in space and time and E is the residual. $k_1 = 2m_1 + 1$ and $k_2 = 2m_2 + 1$ correspond to minimally conforming scalar product space if the space–time integrals in the finite element processes are to be in Riemann sense.

(b) Equation (1) and (a) imply that ${}^n\varphi_h^e \in H^{k,p}({}^n\bar{\Omega}_{xt}^e)$; $k = (k_1, k_2)$, $k_1 \geqslant 2m_1 + 1$, $k_2 \geqslant 2m_2 + 1$ and $p_1 \geqslant 2k_1 - 1$, $p_2 \geqslant 2k_2 - 1$. p_1 and p_2 being the degrees of local approximation of ${}^n\varphi_h^e$ in space and time. Global smoothness of $\varphi_h(x,t)$ of a desired order is due to the global smoothness of ${}^n\varphi_h^e(x,t)$, the local approximation over ${}^n\Omega_{xt}^e$ of the same order [38–40].

DOI: 10.1002/fld

(c) If the theoretical solution $\varphi(x,t)$ is analytic and is of class $C^{L_1,L_2}(\Omega_{xt})$; $2m_1 \leqslant L_1 \leqslant \infty$, $2m_2 \leqslant L_2 \leqslant \infty$, then, $2m_1+1 \leqslant k_1 \leqslant \infty$, $2m_2+1 \leqslant k_2 \leqslant \infty$ must hold in (a) and (b) if $\varphi_h^* \equiv \varphi \ \forall x,t \in \bar{\Omega}_{xt}^{\mathrm{T}}$ in which φ_h^* is the limit point of the sequence of limit points obtained from converging sequences of solutions.

(d) Generally, one limits the global differentiability of $\varphi_h(x,t)$ by choosing $k_1 = \hat{k}_1$ and $k_2 = \hat{k}_2$ such that $2m_1+1 \leqslant \hat{k}_1 \leqslant \hat{L}_1$, $2m_2+1 \leqslant \hat{k}_2 \leqslant \hat{L}_2$. Obviously, choices of $\hat{L}_1$ and $\hat{L}_2$ limit the achievable global smoothness of $\varphi_h(x,t)$. Admissibility of φ_h in $A\varphi - f = 0 \ \forall x,t \in \bar{\Omega}_{xt}^{\mathrm{T}}$ and $\varphi_h^* \to \varphi$ with global differentiability $\hat{L}_1 \geqslant 2m_1+1$ and $\hat{L}_2 \geqslant 2m_2+1$ implies that $2m_1+1 \leqslant k_1 \leqslant \hat{L}_1$, $2m_2+1 \leqslant k_2 \leqslant \hat{L}_2$.

The approximation spaces $H^k(\bar{\Omega}_{xt}^{\mathrm{T}})$ and $H^{k,p}({}^n\bar{\Omega}_{xt}^e)$ for global approximation $\varphi_h(x,t)$ and for local approximation ${}^n\varphi_h^e(x,t)$ are scalar product spaces containing global and local approximation functions of class C^{k-1} for $\bar{\Omega}_{xt}^{\mathrm{T}}$ and ${}^n\bar{\Omega}_{xt}^e$ with standard definition of norms. Here, $k=(k_1,k_2)$, k_1 being the order of the approximation space in space x and k_2, the order of the space in time t. $p=(p_1,p_2)$ in which p_1 and p_2 are degrees of local approximation in space and time. One can easily show that $p_1 \geqslant 2k_1-1$ and $p_2 \geqslant 2k_2-1$.

The orders k_1 and k_2 in space and time of these scalar product spaces yield global differentiability (or smoothness) of orders k_1-1 and k_2-1 in space and time of the approximation $\varphi_h(x,t)$ in $\bar{\Omega}_{xt}^{\mathrm{T}}$. And, that order $k=(k_1,k_2)$ is an independent parameter in all computations for IVP in addition to h and p and hence k-version of finite element for IVP and the associated k, hk, pk and hpk processes in addition to h, p and hp processes.

2.2. Governing differential equation

The viscous form of the transient 1-D Burgers equation in the absence of sources and sinks is given by

$$\frac{\partial \varphi}{\partial t} + \varphi \frac{\partial \varphi}{\partial x} - \frac{1}{Re}\frac{\partial^2 \varphi}{\partial x^2} = 0 \quad \forall (x,t) \in \Omega_{xt} = \Omega_x \times \Omega_t = \Omega_x \times (0,\tau) \tag{2}$$

The boundary conditions (BCs) and initial conditions (ICs) will be discussed in context with specific numerical studies.

For a finite Re, the theoretical solution $\varphi(x,t)$ of (2) is analytic and hence can be expressed as an algebraic polynomial of degrees p_1 and p_2 in space and time in which p_1 and p_2 may be infinity. Hence, $\varphi(x,t)$ is class $c\,c^{p_1,p_2}(\Omega_{xt})$; with $p_1, p_2 = \infty$ is admissible. If $\varphi_h(x,t)$ is an approximation of $\varphi(x,t)$ in $\bar{\Omega}_{xt}^{\mathrm{T}}$, then, we have the following (in space–time, time marching process):

$$\begin{gathered} {}^n\varphi_h^e(x,t) \in H^{k,p}({}^n\bar{\Omega}_{xt}^e), \quad k=(k_1,k_2), \ \ k_1 \geqslant 3 \ \text{ and } \ k_2 \geqslant 2 \\ p_1 \geqslant 2k_1-1 \ \text{ and } \ p_2 \geqslant 2k_2-1 \end{gathered} \tag{3}$$

In (3) $k_1=3$ and $k_2=2$ correspond to the minimally conforming space in space and time if the space–time integrals are to be in Riemann sense. when $k_1=2$ and $k_2=1$, the space–time integrals are in Lebesgue sense. The orders $k_1>3$ and $k_2>2$ are necessitated if $\varphi_h(x,t)$ is to possess the global smoothness up to a desired order which may be desired to incorporate the higher-order global differentiability features of the theoretical solution in the computations and hence, the need for h, p, k framework.

DOI: 10.1002/fld

2.3. Space–time LSP in h, p, k framework

We consider STLSP for (2) over a space–time strip ${}^n\bar{\Omega}_{xt} = \bigcup_{e=1}^{M} {}^n\bar{\Omega}^e_{xt}$ in which ${}^n\bar{\Omega}^e_{xt}$ is a space–time element or sub-domain. Let ${}^n\varphi^e_h(x,t)$ be an approximation of $\varphi(x,t)$ over ${}^n\bar{\Omega}^e_{xt}$ and $V_h({}^n\bar{\Omega}^e_{xt})$ be the approximation space; then,

$$V_h({}^n\bar{\Omega}^e_{xt}) = H^{k,p}({}^n\Omega^e_{xt}), \quad k=(k_1,k_2), \quad p=(p_1,p_2) \ \ \forall {}^n\bar{\Omega}^e_{xt} \in {}^n\bar{\Omega}_{xt} \tag{4}$$

$$H^{(k_1,k_2),(p_1,p_2)}({}^n\bar{\Omega}^e_{xt}) = \{w : w|_{{}^n\bar{\Omega}^e_{xt}} \in c^{(k_1-1,k_2-1),(p_1,p_2)}({}^n\bar{\Omega}^e_{xt}), w|_{{}^n\bar{\Omega}^e_{xt}} \in p^{p_1,p_2}({}^n\bar{\Omega}^e_{xt})$$
$$k_1 \geqslant 3, \ k_2 \geqslant 2, \ p_1 \geqslant 2k_1 - 1, \ p_2 \geqslant 2k_2 - 1 \ \forall {}^n\bar{\Omega}^e_{xt} \in {}^n\bar{\Omega}_{xt}\} \tag{5}$$

${}^n\varphi^e_h(x,t) \in V_h({}^n\bar{\Omega}^e_{xt})$ can be defined using

$$\begin{aligned} {}^n\varphi^e_h(x,t) &= [N^{(k_1-1,k_2-1),(p_1,p_2)}(x,t)]\{{}^n\varphi^e\} \\ &= \sum_{e=1}^{n} N_i(x,t)\,{}^n\varphi^e_i \quad \forall (x,t) \in {}^n\bar{\Omega}^e_h(x,t) \end{aligned} \tag{6}$$

in which $\{{}^n\varphi^e\}$ are nodal degrees of freedom for the space–time element with domain ${}^n\bar{\Omega}^e_{xt}$ and $N^{(k_1-1,k_2-1),(p_1,p_2)}(x,t) \in V_h({}^n\bar{\Omega}^e_{xt})$ are the space–time local approximation functions [43]. With the local approximation ${}^n\varphi^e_h(x,t)$ defined by (6), the STLSP can be described as follows. Find $\{{}^n\varphi_h\} = \bigcup_e \{{}^n\varphi^e_h\}$ such that

$$\delta I({}^n\varphi_h) = \sum_{e=1}^{M} ({}^nE^e, \delta({}^nE^e)) = g({}^n\varphi_h) = 0$$

where

$$I({}^n\varphi_h) = \sum_{e=1}^{M} ({}^nE^e, {}^nE^e)_{{}^n\Omega^e_{xt}}, \quad {}^nE^e = \frac{\partial({}^n\varphi^e_h)}{\partial t} + {}^n\varphi^e_h \frac{\partial({}^n\varphi^e_h)}{\partial x} - \frac{1}{Re}\frac{\partial^2({}^n\varphi^e_h)}{\partial x^2}$$

and

$$\delta^2 I({}^n\varphi_h) \approx \sum_{e=1}^{M} (\delta({}^nE^e), \delta({}^nE^e)) > 0$$

in which

$$\delta({}^nE^e) = \frac{\partial v}{\partial t} + v\frac{\partial({}^n\varphi^e_h)}{\partial x} + {}^n\varphi^e_h \frac{\partial v}{\partial x} - \frac{1}{Re}\frac{\partial^2 v}{\partial x^2}$$

where

$$v = \delta({}^n\varphi^e_h) = N_j(x,t), \quad j = 1, \ldots, n$$

DOI: 10.1002/fld

Using Newton's first-order method with line search to find ${}^n\varphi_h$ iteratively to satisfy $g({}^n\varphi_h)=0$ yields:

$$ {}^n\varphi_h = ({}^n\varphi_h)_0 + \alpha\Delta^n\varphi_h $$

$$ \Delta^n\varphi_h = -[\delta^2 I({}^n\varphi_h)]^{-1}_{({}^n\varphi_h)_0}\{g({}^n\varphi_h)\}_{({}^n\varphi_h)_0} $$

α is determined such that

$$ I({}^n\varphi_h) \leqslant I(({}^n\varphi_h)_0) $$

where $({}^n\varphi_h)_0$ is the assumed or starting solution in the Newton's first-order method.

Remarks

(1) In the STLSP requiring construction of $I({}^n\varphi_h)$ and $\delta I({}^n\varphi_h)=0$, the GDE is not linearized as done by the authors in References [20] and others.
(2) The STLSP is STVC and hence ensures a unique ${}^n\varphi_h$ and unconditionally stable and non-degenerate computational process during time marching and thus the entire evolution.
(3) We note that in the STLSP $I({}^n\varphi_h)$ is minimized by a ${}^n\varphi_h$ that satisfies $\delta I({}^n\varphi_h)=0$ and that minima of $I({}^n\varphi_h)$ is zero. Hence, when $I({}^n\varphi_h)\to 0$ we have ${}^nE^e\to 0$ for $e=1,\ldots,M$ in the point-wise sense. That is convergence of ${}^nE^e$ in L_2-norm yields point-wise convergence of ${}^nE^e$ $\forall(x,t)\in{}^n\bar{\Omega}_{xt}$.
(4) STLSP has the best approximation property in the E-norm, i.e. $\|{}^n\varphi_h\|_E = (\sum({}^nE^e, {}^nE^e)_{{}^n\Omega^e_{xt}})^{1/2}$ is minimum in STLSP compared with any other process.

3. NUMERICAL STUDIES

In this section we present a number of numerical studies to demonstrate the importance of STVC of the space–time integral forms and that of the higher-order spaces in simulating numerical solutions of the transient Burgers equation under various ICs and BCs. The numerical studies are divided into three sections and the model problems used are the same as those used in the published work [3], so that our computed results can be compared with those in References [3]. In all of our computations, viscous form of the Burgers equation is used and hence, the numerical studies are for specific values of *Re* numbers (given with the numerical results). We consider the following three cases for the viscous form of the Burgers equation:

(i) Evolutions and stationary states of a single shock for $Re=100$, 1000 and 10000.
(ii) Evolution and stationary state of a double shock for $Re=1000$.
(iii) Evolution of a transonic shock at $Re=1000$

In all numerical studies time-accurate evolution details as well as the details of the stationary states of the evolutions are presented. For the strong form of the GDE for the Burgers equation, $k_1=3$ and $k_2=2$ correspond to the minimally conforming spaces (ensuring all space–time integral to be Riemann). Actual values of k_1 and k_2 as well as p_1 and p_2 used in the computations are given with the numerical results.

DOI: 10.1002/fld

3.1. Evolution and stationary states of a single shock

The space–time domain $\Omega_{xt} = [0, 1] \times [0, 1]$ is considered in this study with the following ICs and BCs:

$$\text{IC}: \varphi(x, 0) = 0.5, \quad 0 \leqslant x \leqslant 1$$

$$\text{BC}: \varphi(0, t) = \begin{cases} 0.5, & t \leqslant 0.0 \\ 1.0, & t > 0.0 \end{cases}$$

3.1.1. Mathematical representation of step BC and rationale for comparison between theoretical and numerical solutions. From the description of the BC we note that at $t = 0.0$ φ changes from 0.5 to 1.0 (i.e. step function) shown in Figure 1.

From Figure 1 we clearly observe the non-analytic nature of $\varphi(x, t)$ at $t = 0.0$. Let ${}^n\varphi^e(x, t) \in H^{k,p}(\bar{\Omega}^e_{xt})$; $k = (k_1, k_2)$ in which k_2 is the order of the approximation in time. If we assume φ changes from 0.5 to 1.0 over an increment of time Δt in a continuous and differentiable fashion based on the interpolants in the approximation spaces $H^{k,p}(\bar{\Omega}^e_{xt})$, then for progressively increasing k_2 the behavior of $\varphi_h(0, t)$ over Δt (Figure 2) clearly demonstrates that as k_2 increases the distribution of $\varphi_h(0, t)$ becomes steeper and in the limiting case ($k_2 \to \infty$) approaches the step function at $t = \Delta t/2$. Another way to visualize this is that distribution shown in Figure 2 for various values of k_2 are in fact the properties of the distributions shown in Figure 1 in the spaces of progressively higher-order global differentiability in time. From Figure 2 we clearly see that when $k_2 \to \infty$, φ_h remains 0.5 for $0 \leqslant t < \Delta t$ and only attains a value of 1.0 for $t = \Delta t/2$ and thereafter maintains a value of 1.0. Thus, if the theoretical solutions of this model problem were available for BC shown in Figure 3, then when comparing with numerical solutions, one must observe the

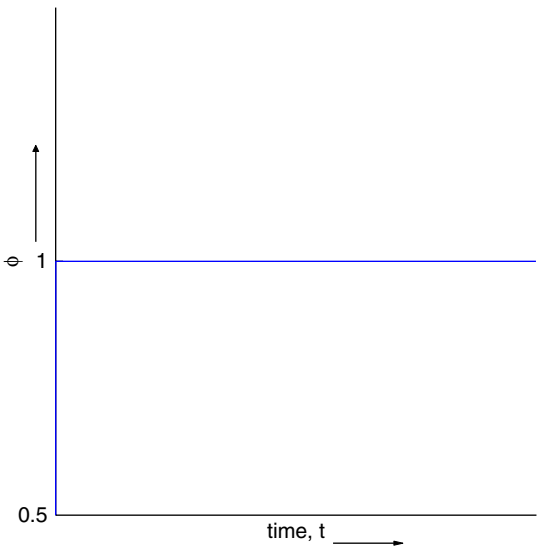

Figure 1. BC at $x = 0$, i.e. $\varphi(0, t)$.

DOI: 10.1002/fld

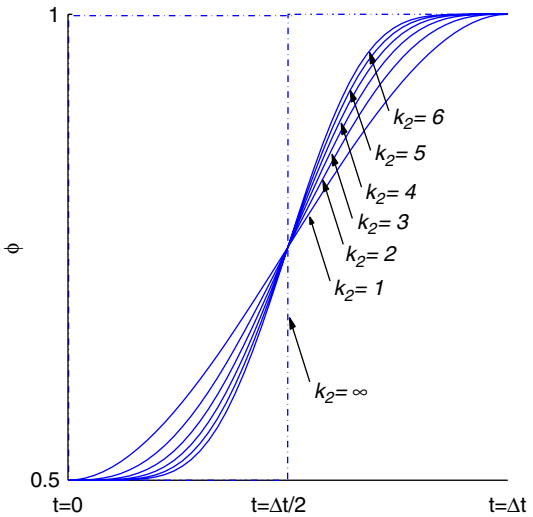

Figure 2. Descriptions of impulsive $\varphi(0,t)$ for $0 \leqslant t \leqslant \Delta t$ in spaces of progressively higher-order global differentiability in time obtained using interpolants.

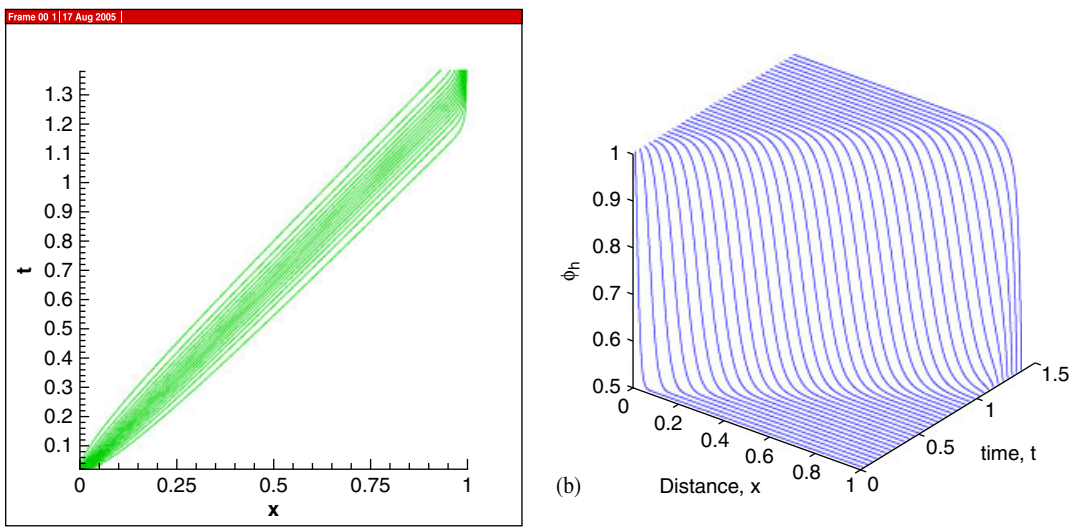

Figure 3. Contours and profiles of φ_h in the x–t domain for a single shock at $Re = 100$: (a) contours of φ_h in the x–t domain and (b) profiles of φ_h in the x–t domain.

following:

$$\varphi(x,t)\|_{t=\Delta t/2} = \varphi_h(x,t)\|_{t=\Delta t}$$

DOI: 10.1002/fld

and

$$\varphi(x,t)\|_{t=\Delta t/2+n\Delta t} = \varphi_h(x,t)\|_{t=\Delta t+n\Delta t} \quad \text{for } n=1,2,\ldots$$

Remarks

(1) As $k_2 \to \infty$ we do achieve impulsive (step change) changes in $\varphi_h(0,t)$ but with a time lag of $\Delta t/2$ (assuming φ_h changes for 0.5 to 1.0 over Δt). This time lag must be taken into account when comparing with theoretical solutions.
(2) Impulsive theoretical nature of $\varphi(0,t)$ at $t=0$ is only realized at high values of k_2, i.e. order of the approximation space in time in the computation at $t=\Delta t/2$ but not at $t=0$.
(3) Figure 2 clearly shows the meritorious nature of ${}^n\varphi_h^e(x,t)$ in $H^{k,p}({}^n\bar{\Omega}_{xt}^e)$ spaces in achieving the desired behavior of $\varphi(0,t)$, at $t=0$. The descriptions of $\varphi(0,t)$ in Figure 1 becomes analytic in $H^{k,p}({}^n\bar{\Omega}_{xt}^e)$ spaces. The representations shown in Figure 2 are using interpolants in various order spaces.
(4) Due to (3) the theoretical solutions of the numerically posed problem in various order spaces in time remain analytic. This aspect permits meaningful numerical simulation in which we can achieve convergence.
(5) In all numerical theoretical studies a step change is simulated over an increment of time Δt with features similar to those shown in Figure 2.
The BC (Figure 2) imposed over Δt evolves into a steady propagating front (shock wave). The speed of the steady front in this case is given by $(\varphi(0,0)+\varphi(0,\Delta t))/2$ which for $\varphi(0,0)$ of 0.5 and $\varphi(0,\Delta t)$ of 1.0 is $\frac{3}{4}$.

3.1.2. Evolution and its stationary state for $Re=100$. Here we consider a single shock at $Re=100$ over $\Omega_{xt}=(0,1)\times(0,1.6)$. The spatial discretization consists of a 50-element uniform mesh over $\bar{\Omega}_x=[0,1]$. The solution is time marched with $\Delta t=0.02$. Since the numerically posed problem (based on Section 3.1.1) has analytic theoretical solution, its numerical solution should pose no problems. We consider solutions of class $C^{1,1}({}^n\bar{\Omega}_{xt}^e)$, i.e. of class C^1 in space as well as time. In this case the integrals in space are in Lebesgue sense but in Riemann sense in time. In this choice the order of the approximation space in x is one order lower than minimally conforming space. We consider $p_1=p_2=11$ (i.e. uniform p-level in space and time). For these choices of h (i.e. $h_t=\Delta t, h_x=\Delta x$), p and k the computed values of g $(=\delta I)$ and the least-squares functional I are $O(10^{-6})$ and $O(10^{-8})$ and the Newton method with line search converges in less than 10 iterations. Such low values of I indicate good accuracy of the computed evolution for each space–time strip. With shock speed of 1.5, the disturbance reaches $x=1$ (end of the spatial domain) at $t=1.33$ but we continue the evolution till the stationary state is achieved. Figure 3(a) and (b) shows contours and profiles of φ_h in x–t space. From Figure 3(a) we observe that due to low Re number (and hence significant physical diffusion) the contours progressively diffuse for progressively increasing values of x and t. Near vertical lines at $x=1.0$ correspond to the stationary state of the evolution. Smooth and oscillation-free profiles of φ_h in Figure 3(b) can be clearly observed. By examining L_2-norms of $\partial\varphi_h/\partial x$ and $\partial\varphi_h/\partial t$ as a function of time for each space–time strip during evolution, a clear assessment of the accuracy of the stationary state of the evolution can be made. Figure 4(a) and (b) plots L_2-norms of $\partial\varphi_h/\partial x$ and $\partial\varphi_h/\partial t$ as a function of time. At or near $t=1.6$, $\|\partial\varphi_h/\partial x\|_{L_2}$ ceases to change and $\|\partial\varphi_h/\partial t\|_{L_2}$ becomes zero, confirming that the evolution has reached the stationary state.

DOI: 10.1002/fld

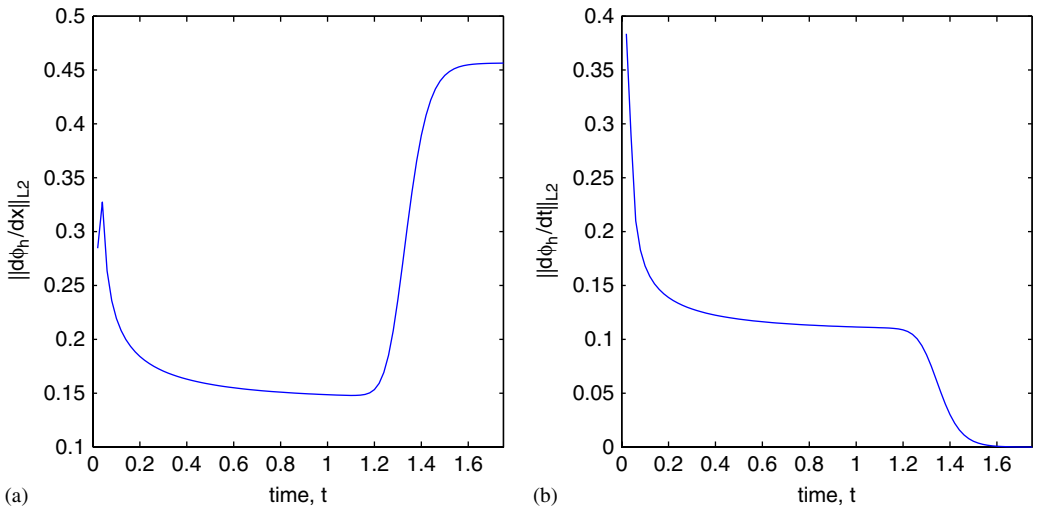

Figure 4. L_2-norms of the $\partial\varphi_h/\partial x$ and $\partial\varphi_h/\partial t$ *versus* time for a single shock at $Re=100$ using space–time strip with time marching: (a) L_2-norm of $\partial\varphi_h/\partial x$ *versus* time and (b) L_2-norm of $\partial\varphi_h/\partial t$ *versus* time.

3.1.3. Evolution and its stationary state for $Re=1000$. At $Re=1000$ the shock width is obviously much smaller compared with $Re=100$. This of course requires a different discretization. Choice of Δt and k_2 depends on how closely we want to approximate non-analytic nature of $\varphi(0,t)$ at $t=0$. These choices influence initial stages of evolution significantly; however, $\varphi_h(x,t)$ during the later stages of evolution is not effected due to the self-correcting nature of the evolution inherent due to non-linear GDE. In this study also we consider solutions of class $C^{1,1}({}^n\bar{\Omega}^e_{xt})$ with $k_1=k_2=2$, $h_x=\Delta x=0.01$, $p_1=p_2=11$ and $h_t=\Delta t=0.01$. Accuracy of g and I similar to those for $Re=100$ (Section 3.1.2) is achieved in this case also and Newton's method with line search also has similar performance. Figure 5(a) and (b) shows contours and profiles of φ_h in x–t space. From Figure 5(a) we observe that due to higher value of Re number (and hence diminished physical diffusion), the contours do not diffuse significantly for progressively increasing values of x and t. Here also, near vertical lines at $x=1.0$ indicate that the evolution has reached stationary state. Smooth and oscillation-free profiles φ_h with higher solution gradients (compared with $Re=100$) can be clearly observed in Figure 5(b). Stationary value of $\|\partial\varphi_h/\partial x\|_{L_2}$ and near-zero value of $\|\partial\varphi_h/\partial t\|_{L_2}$ for $t>1.4$ in the graphs shown in Figure 6(a) and (b) confirm accurate stationary state of the evolution for $t>1.4$.

3.1.4. Evolution and its stationary state for $Re=10\,000$. At this Re number the shock width is even smaller than that for $Re=1000$ (Section 3.1.3). In this study we choose $h_x=\Delta x=0.00125$ and $h_t=\Delta t=0.001$, $k_1=k_2=2$ (i.e. solutions of class $C^{1,1}({}^n\bar{\Omega}^e_{xt})$) and $p_1=p_2=9$. The evolution is obtained by time marching the solution. Accuracy of g and I similar to those in Section 3.1.2 is achieved here as well and Newton's method with line search also performs similarly. Figure 7(a) and (b) shows plots of the contours of φ_h and profiles of φ_h in the x–t domain. From Figure 7(a) we clearly note the consequence of significantly reduced physical diffusion at this Re number,

DOI: 10.1002/fld

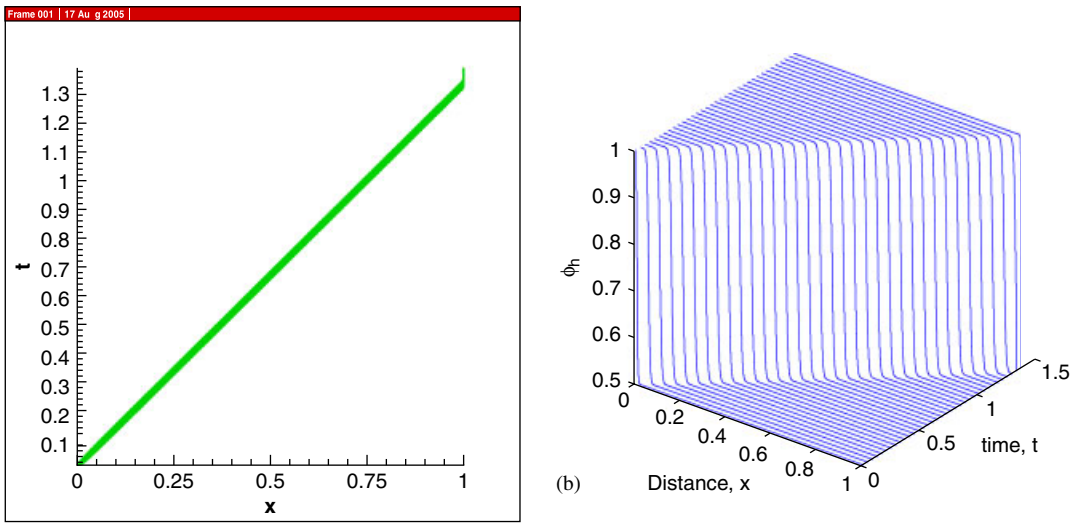

Figure 5. Contours and profiles of φ_h in the x–t domain for a single shock at $Re = 1000$: (a) contours of φ_h in the x–t domain and (b) profiles of φ_h in the x–t domain.

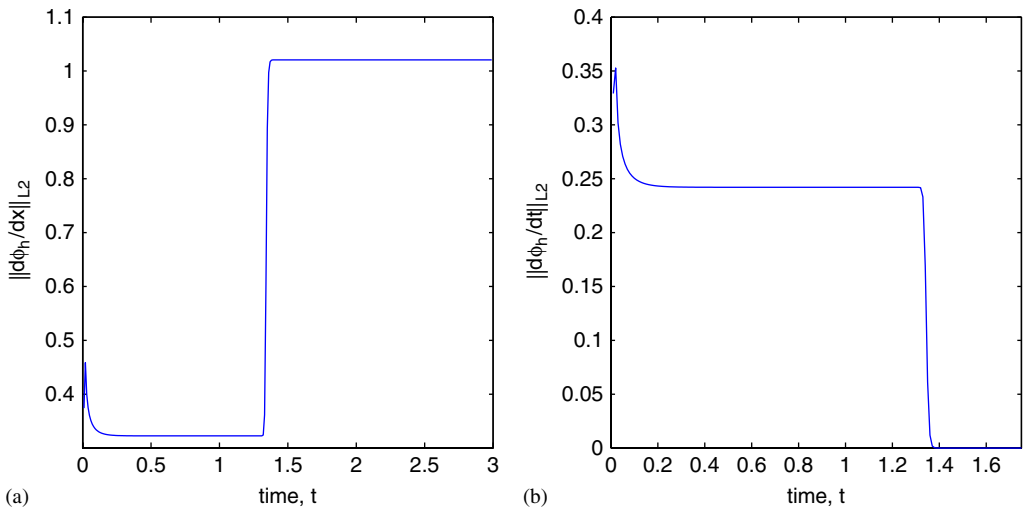

Figure 6. L_2-norms of the $\partial\varphi_h/\partial x$ and $\partial\varphi_h/\partial t$ *versus* time for a single shock at $Re = 1000$ using space–time strip with time marching: (a) L_2-norm of $\partial\varphi_h/\partial x$ *versus* time and (b) L_2-norm of $\partial\varphi_h/\partial t$ *versus* time.

resulting in much narrower width of the contours in the x–t domain. This is obviously due to much isolated and higher solution gradients that are quite clear in Figure 7(b). Profiles of φ_h in Figure 7(b) are smooth and oscillation free. Behaviors of the L_2-norms of $\partial\varphi_h/\partial x$ and $\partial\varphi_h/\partial t$

DOI: 10.1002/fld

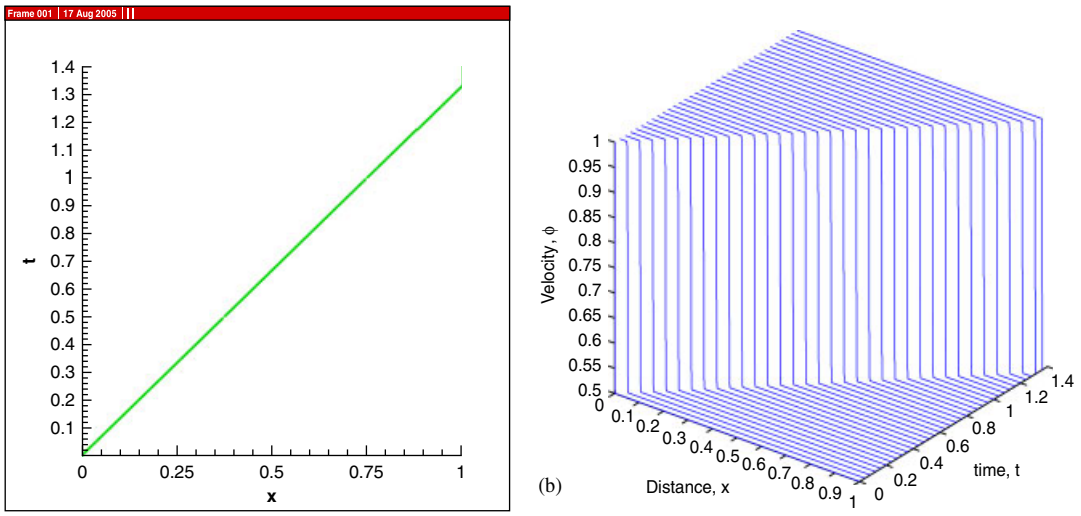

Figure 7. Contours and profiles of φ_h in the x–t domain for a single shock at $Re=10000$: (a) contours of φ_h in the x–t domain and (b) profiles of φ_h in the x–t domain.

versus time similar to those presented in Sections 3.1.2 and 3.1.3 are also observed here (not shown for sake of brevity), confirming the accuracy of the stationary state of the evolution.

3.2. Evolution and stationary state of a double shock at Re=1000.

In this section we consider evolution and stationary state of a double shock over $\Omega_{xt}=(0,2)\times(0,1.6)$ for $Re=1000$ and we consider the following IC and BC:

$$\text{IC}:\varphi(x,0)=\begin{cases}1.5, & 0\leqslant x<0.5\\ 0.5, & 0.5\leqslant x\leqslant 2\end{cases}$$

$$\text{BC}:\varphi(0,t)=\begin{cases}1.5, & t<0\\ 2.5, & t\geqslant 0\end{cases}$$

Figure 8(a) and (b) shows graphs of IC and BC.

We note that IC at $t=0$ is non-analytic due to step change in φ at $x=0.5$ and the BCs at $x=0.0$ is also non-analytic due to step change in φ. In the numerical solutions such behaviors in $H^{k,p}({}^n\bar{\Omega}^e_{xt})$ spaces are represented using interpolants (similar to Figure 2). These representations of Figure 8(a) and (b) are analytic (similar to Figure 2) and as we increase k_1 and k_2, the representations in the respective spaces approach the desired behaviors but always remain analytic and hence the theoretical solutions of the numerically posed double-shock IVP always remains analytic as well. This significant feature permits us to lower the order of approximation spaces below minimally conforming due to the fact that convergence of the lower class solutions to higher class is possible. In this study we consider solutions of class $C^{1,1}({}^n\bar{\Omega}^e_{xt})$ and $C^{2,1}({}^n\bar{\Omega}^e_{xt})$

DOI: 10.1002/fld

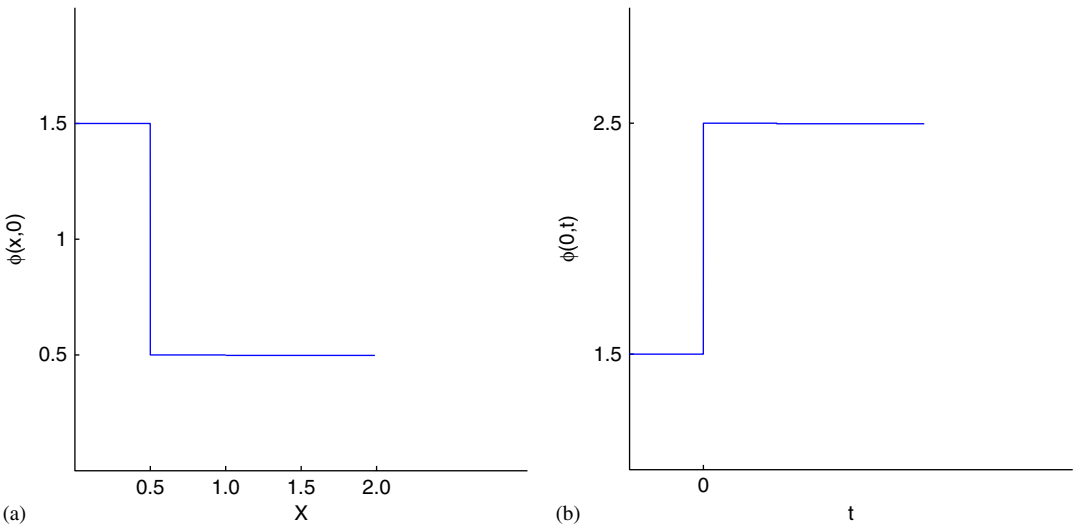

Figure 8. IC and BC for double shock at $Re = 1000$.

to demonstrate the importance of higher order global differentiability in space x. The BC and IC shown in Figure 8 create two disturbances, both of which propagate from left to right but at different speeds and evolve into two shocks. Since the shock due to BC (Figure 8(a)) is traveling at a faster speed than the one due to IC (Figure 8(b)), the two shocks interact and form a single shock that eventually reaches the end of the domain and evolves into stationary state.

In the numerical study presented here we choose $h_x = \Delta x = 0.01$, $p_1 = p_2 = 11$ and $h_t = \Delta t = 0.005$ at $Re = 1000$. First, we consider solution of class $C^{1,1}({}^n\bar{\Omega}^e_{xt})$. Figure 9(a) and (b) shows contours and profiles of φ_h in the x–t domain. From Figure 9(a) shock formations, interaction and subsequent propagation of the resulting shock are clearly observed. Profiles of φ_h in Figure 9(b) remain smooth, oscillation free and clearly show high solution gradients and their accurate resolution. The solution of class $C^{2,1}({}^n\bar{\Omega}^e_{xt})$ were also computed using the same discretization and p-levels as used for solutions of class $C^{1,1}({}^n\bar{\Omega}^e_{xt})$. Figure 10(a) and (b) shows plots of L_2-norms of $\partial\varphi_h/\partial x$ and $\partial\varphi_h/\partial t$ *versus* time t for solutions of classes $C^{1,1}$ and $C^{2,1}$ obtained by using space–time time marching processes. We make the following remarks:

(a) In general, solutions of both classes show good agreement.
(b) In case of solutions of class $C^{1,1}$ $\|\partial\varphi_h/\partial t\|_{L_2}$ becomes constant when evolution ceases but has a finite non-zero value. For local approximation of class $C^{2,1}$, $\|\partial\varphi_h/\partial t\|_{L_2}$ is very close to zero, indicating better accuracy of the stationary state achieved when the local approximations are of class $C^{2,1}$.
(c) Different values of $\|\partial\varphi_h/\partial x\|_{L_2}$ for the two classes of solution for $t > 1.2$ are clearly seen as well.
(d) Exploded views in Figure 1(a) and (b) show oscillatory behaviors of both L_2-norms when the local approximations are of class $C^{1,1}$ but free of oscillations for the solution of class $C^{2,1}$.

DOI: 10.1002/fld

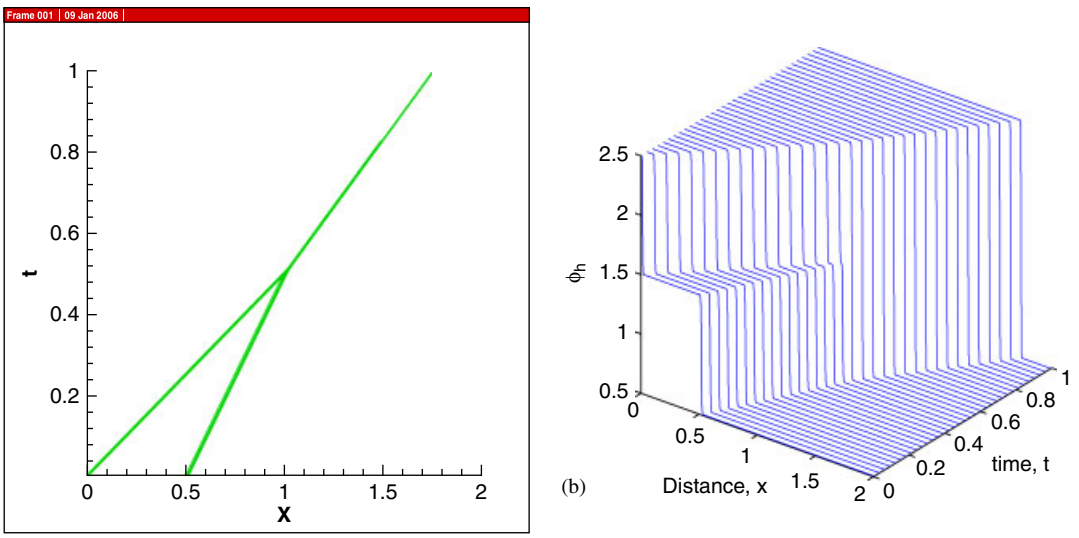

Figure 9. Contours and profiles of φ_h in the x–t domain for a double shock at $Re=1000$: (a) contours of φ_h in the x–t domain and (b) profiles of φ_h in the x–t domain.

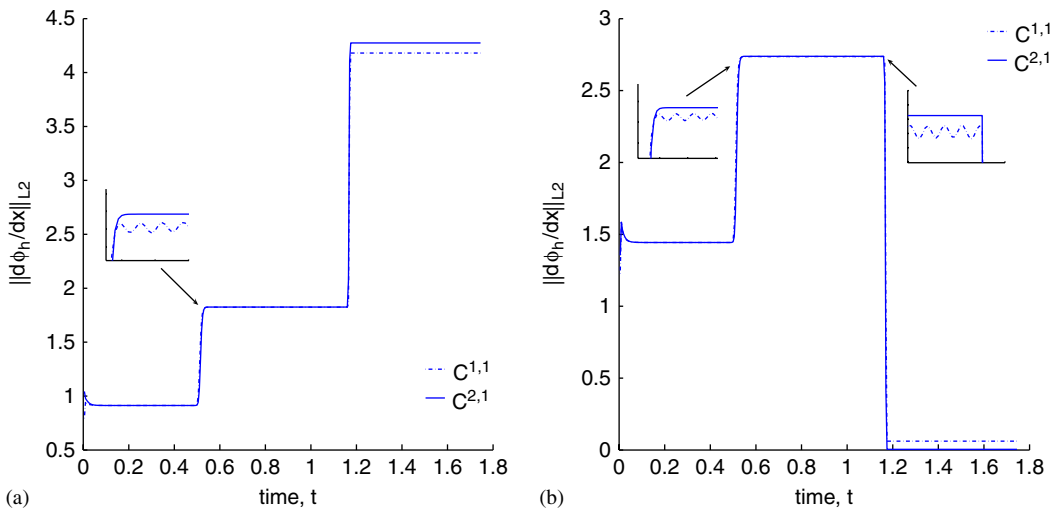

Figure 10. L_2-norms of the $\partial\varphi_h/\partial x$ and $\partial\varphi_h/\partial t$ for solutions of classes $C^{1,1}$ and $C^{2,1}$ for double shock at $Re=1000$: L_2-norm of $\partial\varphi_h/\partial x$ *versus* time and (b) L_2-norm of $\partial\varphi_h/\partial t$ *versus* time.

(e) Solutions of class $C^{2,1}({}^n\bar{\Omega}^e_{xy})$ correspond to $k_1=3$ and $k_2=2$, which is the minimally conforming space for the model problem. Superiority of the solutions of classes $C^{2,1}$ over those of $C^{1,1}$ is clearly observed.

DOI: 10.1002/fld

3.3. Evolution of transonic shock at Re = 1000

In this section we consider a transonic shock problem described by the following ICs and BCs:

$$\text{IC}: u(x,0) = \begin{cases} -0.5, & -1 \leqslant x < 0 \\ 2.5, & 0 < x \leqslant 1.5 \end{cases}$$

$$\text{BC}: u(0,t) = -0.5 \quad \forall t \in [0, \tau]$$

In this case we note that BC data do not have discontinuity but the IC data shown in Figure 11(a) are non-analytic. As in the previous model problems, here also we regularize IC using interpolants over $h_x = \Delta x$. The domain of definitions $\Omega_{xt} = (-1, 1.5) \times (0, 3.0)$ is discretized using $h_x = \Delta x = 0.0125$ and $h_t = \Delta t = 0.005$. We consider local approximations of class $C^{1,1}({}^n\bar{\Omega}^e_{xy})$ corresponding to $k_1 = k_2 = 2$ and we choose $p_1 = p_2 = 9$. The evolution is time marched using space–time strip. The values of g and $I({}^n\varphi_h)$ remain $O(10^{-6})$ and $O(10^{-8}$ during the entire evolution, indicating convergence of Newton's method with line search and good accuracy of the evolution. Figure 12(a) and (b) shows contours and profiles of φ_h in the x–t domain. Evolutions are oscillation free and smooth. Evolution of rarefaction is simulated quite well as time elapses. Profiles of φ_h shown in Figure 12(b) indicate that gradients of φ_h are preserved and solutions are oscillation free as well. Owing to rarefaction (i.e. diffusion) the stationary state of the evolution will require a much larger value of time. This is quite obvious from the graphs of L_2-norms of $\partial\varphi_h/\partial x$ and $\partial\varphi_h/\partial t$ *versus* time t shown in Figure 13. Even at $t = 3.0$, L_2-norm of the $\partial\varphi_h/\partial x$ has not reached a steady value and L_2-norm of the $\partial\varphi_h/\partial t$ continues to decrease but has not reached zero (numerically computed) value.

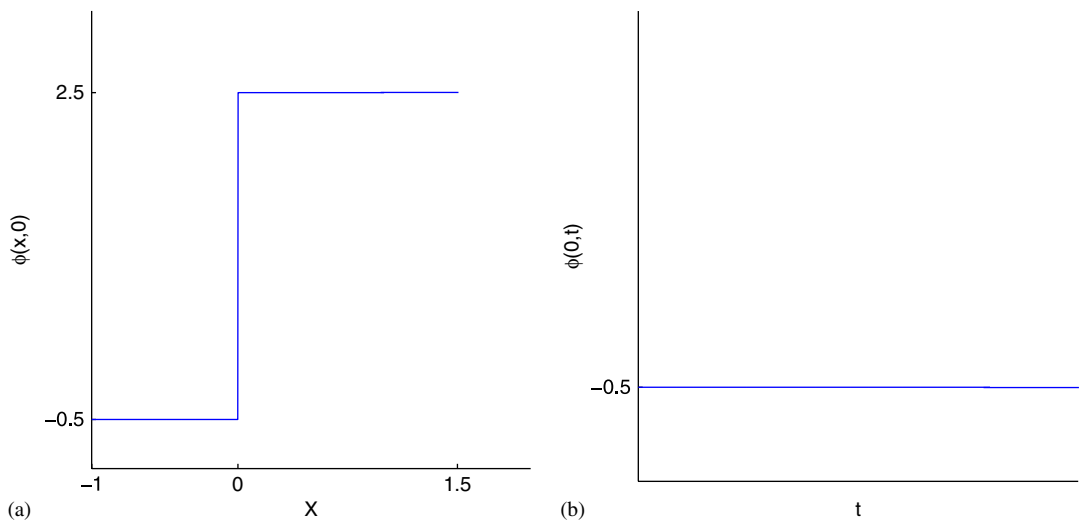

Figure 11. IC and BC for transonic shock at $Re = 1000$.

DOI: 10.1002/fld

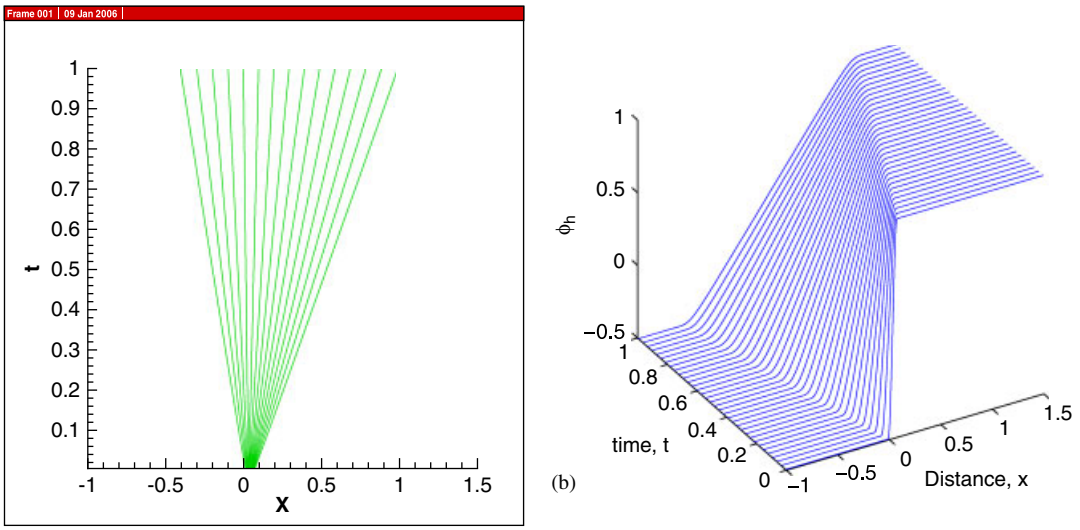

Figure 12. Contours and profiles of φ_h in the x–t domain for a transonic shock at $Re = 1000$: (a) contours of φ_h in the x–t domain and (b) profiles of φ_h in the x–t domain.

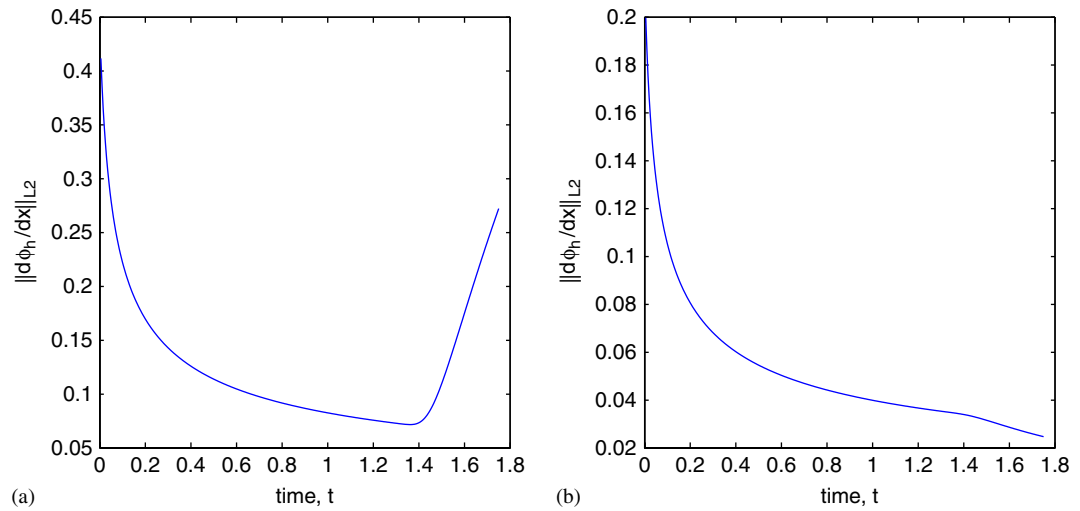

Figure 13. L_2-norms of the $\partial\varphi_h/\partial x$ and $\partial\varphi_h/\partial t$ for transonic shock problem at $Re = 1000$: (a) L_2-norm of $\partial\varphi_h/\partial x$ *versus* time and (b) L_2-norm of $\partial\varphi_h/\partial t$ *versus* time.

3.4. Evolutions for progressively increasing CFL numbers: unconditional non-degeneracy and stability of STLSP

Numerical studies are presented in this section to demonstrate: (i) The STLSP are unconditionally non-degenerate, i.e. computations are possible for any choices of h, p and k; (ii) to show that even

DOI: 10.1002/fld

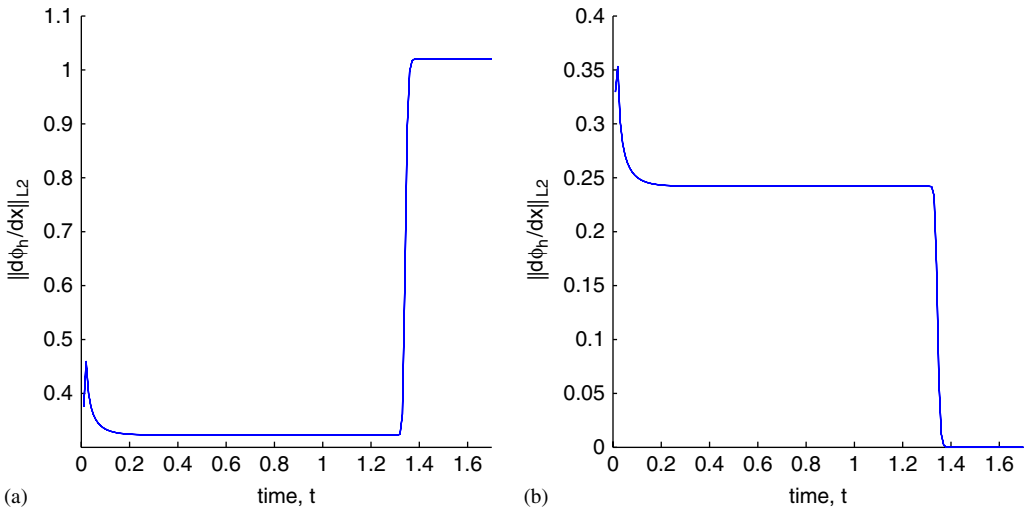

Figure 14. L_2-norms of the $\partial\varphi_h/\partial x$ and $\partial\varphi_h/\partial t$ for meshes of 200, 400, 800 elements in space with $h_t = \Delta t = 0.01$ and $Re = 1000$: (a) L_2-norm of $\partial\varphi_h/\partial x$ *versus* time and (b) L_2-norm of $\partial\varphi_h/\partial t$ *versus* time.

though the CFL number does influence accuracy the STLSP are unconditionally stable; (iii) good accuracy of evolution is achievable for very high CFL numbers. We consider the model problem with a single shock at $Re = 1000$ (Section 3.1.3). Numerical studies were conducted using space–time strip with time marching for 200, 400 and 800 element uniform discretizations in spatial domain using $h_t = \Delta t = 0.01$, which correspond to CFL numbers of 2, 4 and 8. $k_1 = k_2 = 2$ and $p_1 = p_2 = 9$ were chosen. For these values of the computational parameters, g and $I({}^n\varphi_h)$ were $O(10^{-10})$ and $O(10^{-7})$ for all space–time strips for three values of the CFL numbers. Figure 14(a) and (b) shows that L_2-norms of $\partial\varphi_h/\partial x$ and $\partial\varphi_h/\partial t$ *versus* time are indistinguishable from each other for all three values of CFL numbers.

4. SUMMARY AND CONCLUSIONS

The mathematical and computation aspects as well as numerical studies in *hpk* framework are presented for time-dependent partial differential equation resulting from a single non-linear conservation law. Viscous form of the Burgers equation is used as a specific model problem. A summary of the work and the conclusions are given in the following.

(1) The viscous form of the Burgers equation containing highest-order derivatives of the dependent variable (as opposed to a system of first-order equations) is used in the space–time least-squares finite element formulation as well as the numerical studies.
(2) GDE is not linearized prior to constructing the least-squares functional as done in Reference [3] and other published works. The merits of this approach are: (a) the least-squares functional and its first variation correspond to the precise non-linear mathematical model. (b) In this simple model problem, the linearization of GDE may be obvious but in the case

DOI: 10.1002/fld

of more complex physics (such as Navier–Stokes equations) this may not be the case. (c) Newton's method with line search is only employed while solving the non-linear algebraic equations resulting from the first variation of least-squares functional set to zero. (d) This approach is free of assumptions, approximations and is applicable to all non-linear partial differential equations.

(3) The space–time local approximations are in higher-order approximation spaces which permit higher-order global differentiability of the approximations in space as well as time. The order k of the approximation space is an independent parameter in addition to h and p. Use of higher-order spaces permit use of GDE containing the higher-order derivatives of the dependent variables in the integral forms as well as allow us to incorporate the desired global differentiability features of the theoretical solutions in the design of the computational process.

(4) For the model considered here the space–time strip with time marching is utilized as opposed to space–time meshes [3]. This is computationally efficient and permits control of approximation errors due to the fact that the evolution is not time marched until the converged solution is obtained for the current space–time strip.

(5) In case of a single shock (Section 3.1), numerical studies for progressively increasing Re numbers demonstrate: (a) smooth evolutions; (b) accurate stationary state; and (c) progressively reduced shock width for progressively increasing Re number. As $Re \to \infty$, the singular solutions of the inviscid form of the Burgers equation are approached. Similar features exist for the double shock also (Section 3.2), even though the numerical study in the paper is only for $Re = 1000$. Simulation of transonic shock at $Re = 1000$ (Section 3.3) presents no difficulties. Evolution is smooth and oscillation free. Significantly low values of least-squares functional $I = O(10^{-8})$ or lower ones for all space–time strips indicate that GDE is satisfied accurately in the point-wise sense during the entire evolution and hence all evolutions presented here are very close to being time accurate. Space–time least-squares functional converges monotonically and remains bounded for all choices of hpk.

(6) It is worth reiterating that solutions of inviscid Burgers equation are singular, hence non-analytic and thus non-unique [1]. As pointed out in Reference [1], the theory of generalized solutions leads to non-uniqueness when applied to the inviscid Burgers equation and the only means of restoring uniqueness is to incorporate viscous mechanism. Thus, all approaches and methodologies dealing with numerical solutions of inviscid Burgers equation are based on addition of artificial diffusion to the inviscid form and then demonstrating its vanishing nature in some limiting process. Secondly, the viscous mechanism in these approaches may not be in precise agreement with the physics of diffusion present in the viscous form of Burgers equation. Thus, the numerical solutions obtained from artificial viscosity approach may or may not correspond to that of the viscous form with a specific value of Re. This obviously raises the question of time accuracy of the evolutions in artificial diffusion approaches.

(7) In the approach presented here using viscous form of the Burgers equation, the time-accurate evolutions and their stationary state can be and has been established precisely for specific Re numbers and as $Re \to \infty$ the vanishing nature of the shock width is quite clear from the numerical studies presented here. In this approach the solution remains analytic, associated functionals exhibit monotonic convergence and the computational processes remain unconditionally stable and non-degenerate. The STLSP for Burgers equation is constructed in a straightforward manner without linearization, any assumption or approximations.

DOI: 10.1002/fld

Up-winding methods or any other *ad hoc* treatments are neither needed nor used in the work presented here.

ACKNOWLEDGEMENTS

This research work has been sponsored by grants from DEPSCoR, AFOSR and WPAFB under grant numbers F49620-03-1-0298 and F49620-03-1-0201. The support provided by the first and the third authors' endowed professorships is gratefully acknowledged. The computational facilities provided by CML (Computational Mechanics Laboratory) of the Department of Mechanical Engineering of the University of Kansas are also acknowledged.

REFERENCES

1. Godunov SK. The problem of a generalized solution in the theory of quasilinear equations and in gas dynamics. *Russian Mathematical Surveys* 1962; **17**(3):145–146.
2. Rozhdestvenskii BL. Discontinuous solution of hyperbolic systems of quasilinear equations. *Russian Mathematical Surveys* 1960; **15**(6):53–111.
3. De Sterck H, Manteuffel TA, McCormick SF, Olson L. Numerical conservation properties of H(div)-conforming least-squares finite element methods for the Burgers equation. *SIAM Journal on Scientific Computing* 2005; **26**(5):1573–1597.
4. Grimm JL. Solutions in the large for nonlinear hyperbolic systems of equations. *Communications on Pure and Applied Mathematics* 1965; **18**:697–715.
5. Smoller JA. On the solution of the Riemann problem with general step data for and extended class of hyperbolic systems. *Communications on Pure and Applied Mechanics* 1970; **23**:791–801.
6. Smoller JA. Contact discontinuities in quasi-linear hyperbolic systems. *Communications on Pure and Applied Mathematics* 1970; **23**:791–801.
7. Hopf E. On the right weak solution of Cauchy problem for a quasilinear equation of first order. *Journal of Mathematics and Mechanics* 1969; **19**(6):483–487.
8. Friedrichs KO, Lax PD. Systems of conservation equations with a convex extension. *Proceedings of the National Academy Sciences of United States of America* 1971; **68**(8):1686–1688.
9. Kruzhkov SN. First order quasilinear equations in several variables. *Mathematics of the USSR Shornik* 1970; **10**(2).
10. Mock MS. Discrete shocks and genuine nonlinearity. *Michigan Mathematical Journal* 1978; **25**:131–146.
11. Mock MS. On fourth-order dissipation and single conservation laws. *Communication on Pure and Applied Mathematics* 1976; **29**:383–388.
12. Diperna RJ. Uniqueness of solutions to hyperbolic conservation laws. *Indiana University Mathematics Journal* 1979; **28**(1):137–188.
13. Keyfitz BL, Kranzer HC. Existence and uniqueness of entropy solutions to the Riemann problem for hyperbolic systems of two nonlinear conservation laws. *Journal of Differential Equations* 1978; **27**:444–476.
14. Noh WF. Errors for calculations of strong shocks using an artificial viscosity and an artificial heat flux. *Journal of Computational Physics* 1978; **72**:78–120.
15. Rayleigh L. Aerial plane waves of finite amplitude. *Proceedings of the Royal Statistical Society, Series A* 1910; **84**:247–284.
16. Menikoff R. Errors when shock waves interact due to numerical shock width. *SIAM Journal on Scientific Computing* 1994; **15**(5):1227–1242.
17. Winterscheidt D, Surana KS. p-Version least squares finite element formulation for convection–diffusion problems. *International Journal for Numerical Methods in Engineering* 1993; **36**:111–122.
18. Winterscheidt D, Surana KS. p-Version least squares finite element formulation for Burgers equation. *International Journal for Numerical Methods in Engineering* 1993; **36**:3629–3646.
19. Fiard JM, Manteuffel TA, McCormick SF. First-order system least squares (FOSLS) for convection–diffusion problems: numerical results. *SIAM Journal on Scientific Computing* 1998; **19**(6):1958–1979.
20. Cai Z, Manteuffel TA, Mccormick SF, Ruge J. First-order system LL (FOSLL*): scalar elliptic partial differential equations. *SIAM Journal on Numerical Analysis* 2001; **39**(4):1418–1445.

DOI: 10.1002/fld

21. Strang G. Variational crimes in finite element method. *Annals of Mathematics Study*, vol. 33. Princeton University Press: Princeton, NJ, 1954.
22. Baseley G, Cheng Y, Irons B, Zienkiewicz OC. Triangular elements in bending conforming and nonconforming solutions. *Conference on Matrix Methods*. AFIT: Wright-Patterson, OH, 1965.
23. Carey GF, Oden JT. *Finite Elements*: *A Second Course*, vol. 2. Prentice-Hall: Englewood Cliffs, NJ, 1983.
24. Oden JT, Carey GF. *Finite Elements*: *Mathematical Aspects*. Prentice-Hall, Englewood Cliffs, NJ, 1983.
25. Patera J, Pettman FT. Isoparametric Hermite elements. *International Journal for Numerical Methods in Engineering* 1994; **37**:3489–3519.
26. Katz N, Wang DW. The p-version of finite element method requiring C^1-continuity. *SIAM Journal on Numerical Analysis* 1985; **22**(6):1082–1106.
27. Wang DW, Katz IN, Szabo BA. *Implementation of C^1 Triangular Element Based on the p-version of the Finite Element Method*. NASA Conference Publication, vol. 2245. Research on Structural and Solid Mechanics, 1982; 153–170. *Computers and Structures* 1984; **19**(3):381–392.
28. Wang DW. The *p*-version of the finite element methods for problems requiring C^1-continuity. *Doctoral Dissertation*. Department of Systems Science and Mathematics, Washington University, 1982.
29. Irons BM. A conforming quartic triangular element for plate bending. *International Journal for Numerical Methods in Engineering* 1969; **1**:29–45.
30. Morgan J, Scott R. A nodal basis for C^1 piecewise polynomials of degree $n \geqslant 5$. *Mathematics and Computation* 1975; **29**:736–740.
31. Peano AG. Hierarchies of conforming finite elements for plane elasticity and plate bending. *Computers and Mathematics with Applications* 1976; **2**:221–224.
32. Zienkiewicz OC, Taylor RL, Too JM. Reduced integration technique in general analysis of plates and shells. *International Journal for Numerical Methods in Engineering* 1971; **1**:275–320.
33. Surana KS, Van Dyne DG. Non-weak/strong solutions in gas dynamics: a C^{11} *p*-Version STLSFEF in Lagrangian frame of reference using ρ, u, T primitive variables. *International Journal of Computational Science and Engineering* 2001; **2**(3):357–382.
34. Surana KS, Van Dyne DG. Non-weak/strong solutions in gas dynamics: a C^{11} *p*-version STLSFEF in Eulerian frame of reference using ρ, u, T primitive variables. *International Journal of Computational Science and Engineering* 2001; **2**(3):383–483.
35. Surana KS, Van Dyne DG. Non-weak/strong solutions in gas dynamics: a C^{11} *p*-version STLSFEF in Lagrangian frame of reference using ρ, u, P primitive variables. *International Journal of Computational Science and Engineering* 2001; **2**(3):1025–1050.
36. Surana KS, Van Dyne DG. Non-weak/strong solutions in gas dynamics: a C^{11} *p*-version STLSFEF in Lagrangian frame of reference using ρ, u, P primitive variables. *International Journal of Computational Science and Engineering* 2001; **2**(3):1051–1099.
37. Nayak HV. Solutions of classes C^{00} and C^{11} for two dimensional Newtonian and polymer flows. *Ph.D. Dissertation*, University of Kansas, 2001.
38. Surana KS, Bona M. Non-weak/strong solutions of linear and non-linear hyperbolic and parabolic equations resulting from a single conservative law. *International Journal of Computational Science and Engineering* 2000; **1**(2):299–330.
39. Surana KS, Ahmadi A, Reddy JN. *k*-Version of finite element method for self-adjoint operators in B.V.P. *International Journal of Computational Science and Engineering* 2002; **3**(2):155–218.
40. Surana KS, Ahmadi A, Reddy JN. *k*-Version of finite element method for non-self-adjoint operators in B.V.P. *International Journal of Computational Science and Engineering* 2004; **4**(4):737–812.
41. Surana KS, Ahmadi A, Reddy JN. *k*-Version of finite element method for non-linear operators in B.V.P. *International Journal of Computational Science and Engineering* 2004; **5**(1):133–207.
42. Surana KS, Allu S, Tenpas PW, Reddy JN. *k*-Version of finite element method in gas dynamics: higher order global differentiability numerical solutions. *International Journal for Numerical Methods in Engineering* 2007; **69**(6):1109–1157.
43. Surana KS, Allu S, Reddy JN. The *k*-version of finite element method for I.V.P. Part I: mathematical and computational framework. *International Journal of Computational Engineering Science and Mechanics* 2007; **8**(3):123–136.

DOI: 10.1002/fld